



Influence of inclined magnetic field and chemical reaction on the entropy generation of Blasius and Sakiadis flows

Abiodun A. Opanuga*, Olasumbo O. Agboola, Hilary I. Okagbue, Peter O. Ogunniyi

Department of Mathematics, Covenant University, Ota, Nigeria

ARTICLE INFO

Article history:

Received 5 August 2020

Revised 30 October 2020

Accepted 13 November 2020

Keyword:

Blasius flow

Sakiadis flow

Entropy generation

Chemical reaction

Runge-Kutta method

ABSTRACT

This work considers the well-known laminar boundary layer flows; about a flat-plate in a uniform stream of fluid (Blasius flow) and about a moving plate in a quiescent ambient fluid (Sakiadis flow) both under a convective surface boundary condition. Entropy generation due to the effect of angle of inclination, magnetic parameter, chemical reaction parameter and Schmidt number on the flows is investigated. The third order partial differential equations governing the flows are reduced to ordinary differential equations by suitable similarity variables. The obtained equations are tackled by the Runge-Kutta fourth order method with shooting technique and the results are employed to calculate entropy generation. The solution of Blasius flow is compared with the works in literature and are found to be in excellent agreement. Entropy generation can be minimized by increasing the magnetic parameter (M), chemical reaction parameter (R) and Schmidt number (Sc) for Blasius flow. Magnetic parameter reduces entropy generation for Sakiadis flow while other parameters such as angle of inclination, chemical reaction parameter and Schmidt number boost fluid irreversibility.

© 2020 The Authors. Published by Elsevier B.V. on behalf of African Institute of Mathematical Sciences / Next Einstein Initiative.

This is an open access article under the CC BY license (<http://creativecommons.org/licenses/by/4.0/>)

Introduction

The classical Blasius and Sakiadis flows have been widely investigated by several researchers in the recent years because of their significant applications in several engineering and industrial processes such as polymer extrusion, drawing of copper wires, continuous stretching of plastic films and artificial fibers, wire drawing, glass-fiber, metal extrusion, and metal spinning. The flow along a horizontal, stationary surface located in a uniform free stream was first investigated by Blasius [1] in 1908 while Sakiadis [2] analyzed the flow of a boundary layer on a mobile surface with constant velocity. Although the equations obtained by both researchers are similar the boundary conditions are not the same. In 1938 Howarth [3] applied the Runge-Kutta method to reinvestigate the Blasius problem. Further analysis was carried out by Abussita [4] to establish the validity of the solution. The heat transfer through laminar boundary layer was investigated by Lighthill [5]. Tsou et al. [6] further investigated the Sakiadis flow. The effect of suction/injection on a moving plate inside a free stream for both

* Corresponding author.

E-mail address: abiodun.opanuga@covenantuniversity.edu.ng (A.A. Opanuga).

Nomenclature

u, v	velocity components along x and y directions respectively
U_∞	Constant free stream velocity
U_w	plate velocity
ν	kinematic viscosity
k	thermal conductivity
c_p	specific heat of the fluid at constant pressure
ρ	fluid density
g	acceleration due to gravity
μ	dynamic viscosity
T	temperature of the fluid
B_0^2	magnetic field parameter
β	thermal expansion coefficient
β_c	solutal expansion coefficient
α	thermal diffusivity
D	coefficient of mass diffusivity
B_i	Biot number

Blasius and Sakiadis flows was considered by Chen [7]. Further investigations include the influence of thermal radiation and convective heat boundary conditions [8–14], effect of velocity slip boundary condition [15] and hydromagnetic effect [16,17].

Several important phenomenon occurring in nature and those industrial and engineering processes have necessitated the investigation of simultaneous heat and mass transfer. An in-depth understanding of processes such as evaporation, condensation, sublimation, solution mining of salt caverns for crude oil storage, casting of metal alloys and photosynthesis, solidification of binary alloy and crystal growth, melting and cooling near ice surfaces is required to properly monitor the interaction between the thermal and solutal buoyance forces. The heat transfer analysis has been undertaken by several researchers Waqas [18], Waqas et al. [19–21], Hayat [22,23]. Furthermore, investigation regarding heat and mass transfer of a laminar boundary layer flow has been conducted by a number of authors; Subhashini et.al. [24], Reddaiah and Rao [25], Olanrewaju et.al. [26], Hayat et al. [27] and Irfan et al. [28].

However, several thermal and industrial systems are not efficient due to irreversibility which usually arises during such processes. An irreversible process occurs when both the system and its surrounding cannot be returned to its original state. Processes such as fluid friction, heat transfer, magnetohydrodynamic, thermal radiation have been found to be generating irreversibilities. Since irreversibility promotes entropy generation which is a destruction of the quality of available energy. Improving the quality of useful energy in a fluid flow is of utmost importance and this can be achieved by examining the distribution of entropy generation within the flow field. This is possible by adjusting some fluid thermophysical parameters which encourage entropy production within that region. The approach by Bejan [29,30] revealed that minimization of entropy production will improve thermal systems and designs. Thereafter the approach has been adopted by several other investigators [23–39].

This work aims at exploring the irreversibility associated with laminar boundary layer about a flat-plate in a uniform stream of fluid (Blasius flow) and about a mobile plate in a quiescent ambient fluid (Sakiadis flow). Inclined magnetic field and chemical reaction effects on entropy generation which have not been accounted for in literature are examined in this work. The significance of this work is found in several natural phenomena and engineering processes where the coupling of fluid velocity, thermal and concentration fields is unavoidable. These include crude oil storage, casting of metal alloys, photosynthesis, cooling metallic plates in cooling baths, growing crystals. The Blasius and Sakiadis flows equations have been approximated by some researchers by applying several techniques like Laguerre function collocation method [40], Numerical quasilinearization scheme [41], LTNHPM [42], Quartic B-spline method [43], Taylor series method [44]. Runge-Kutta method which has been applied by some authors [26,45,46] is employed in this work due to its high accuracy and rapid convergence.

Problem statement

Consider a two dimensional mixed convection boundary layer flow of an incompressible, viscous and electrically conducting fluid with a constant free stream velocity U_∞ and U_w as the plate velocity. An inclined magnetic field at angle γ to the fluid flow is applied. Choosing the Cartesian coordinates (x, y) such that x – axis is along the plate while y – axis is normal to the plate. The induced magnetic field is neglected due to the assumption that it is small compared to the applied magnetic field. Furthermore, for the Blasius case, the variable free stream velocity is taken as $U(x) = ax$ while the linear stretching velocity is $U(x) = ax$ for the Sakiadis case, see Fig. 1. Buoyancy forces are induced due to the density variation of temperature and concentration and as such incorporated in the momentum equation. Following the assumptions made, the governing equations are [11,46]

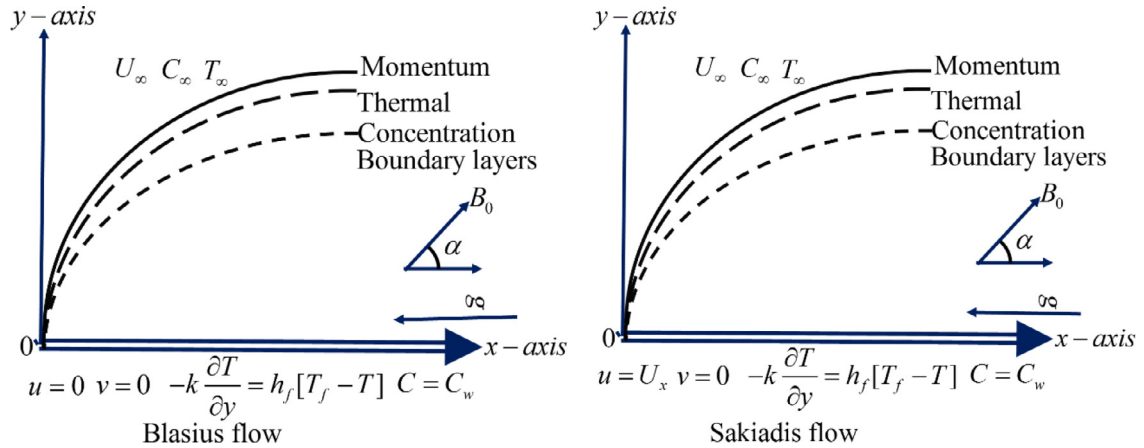


Fig. 1. Flow configuration and coordinate system.

$$\frac{\partial u}{\partial x} + \frac{\partial v}{\partial y} = 0, \tag{1}$$

$$u \frac{\partial u}{\partial x} + v \frac{\partial u}{\partial y} = \nu \frac{\partial^2 u}{\partial y^2} - \frac{\sigma B_0^2 u}{\rho} \sin^2(\gamma) + g\beta(T - T_\infty) + g\beta^*(C - C_\infty), \tag{2}$$

$$u \frac{\partial T}{\partial x} + v \frac{\partial T}{\partial y} = \alpha \frac{\partial^2 T}{\partial y^2} + \frac{\mu}{\rho c_p} \left(\frac{\partial u}{\partial y} \right)^2, \tag{3}$$

$$u \frac{\partial C}{\partial x} + v \frac{\partial C}{\partial y} = D \frac{\partial^2 C}{\partial y^2} + R_1(C - C_\infty). \tag{4}$$

The following boundary conditions are imposed,

$$\left. \begin{aligned} u(0) = 0, v = 0, -k \frac{\partial T}{\partial y}(0) = h_f [T_f - T], C = C_w, \\ u(\infty) \rightarrow U(x) = ax, T(\infty) \rightarrow T_\infty, C(\infty) \rightarrow C_\infty. \end{aligned} \right\} \text{Blasiusflow} \tag{5}$$

$$\left. \begin{aligned} u(0) = U(x) = ax, v = 0, -k \frac{\partial T}{\partial y}(0) = h_f [T_f - T], C = C_w, \\ u(\infty) \rightarrow 0, T(\infty) \rightarrow T_\infty, C(\infty) \rightarrow C_\infty. \end{aligned} \right\} \text{Sakiadisflow} \tag{6}$$

To obtain the similarity equations together with the boundary conditions, the following similarity transformation variables are applied,

$$\eta = y \left(\frac{U_\infty}{\nu x} \right), u = U_\infty f'(\eta), v = \frac{1}{2} \left(\frac{U_\infty \nu}{x} \right) (\eta f' - f), \theta = \frac{T - T_\infty}{T_f - T_\infty}, \phi = \frac{C - C_\infty}{C_w - C_\infty}. \tag{7}$$

On the application of Eq. (7), the dimensionless coupled ordinary differential equations are obtained as,

$$\frac{d^3 f}{d\eta^3}(\eta) + \frac{1}{2} f(\eta) \frac{d^2 f}{d\eta^2}(\eta) - M^2 \sin^2(\gamma) \frac{df}{d\eta}(\eta) + Gr\theta(\eta) + Gc\phi(\eta) = 0, \tag{8}$$

$$\frac{1}{Pr} \frac{d^2 \theta}{d\eta^2}(\eta) + \frac{1}{2} f(\eta) \frac{d\theta}{d\eta}(\eta) + Ec \left(\frac{d^2 f}{d\eta^2}(\eta) \right)^2 = 0, \tag{9}$$

$$\frac{1}{Sc} \frac{d^2 \phi}{d\eta^2}(\eta) + \frac{1}{2} f(\eta) \frac{d\phi}{d\eta}(\eta) - R\phi(\eta) = 0. \tag{10}$$

The boundary conditions for the Blasius and Sakiadis flows are respectively given as;

$$\left. \begin{aligned} f(0) = 0, \frac{df}{d\eta}(0) = 0, \frac{df}{d\eta}(\infty) \rightarrow 1, \\ \frac{d\theta}{d\eta}(0) = -Bi[1 - \theta(0)], \theta(\infty) \rightarrow 0, \phi(0) = 1, \phi(\infty) \rightarrow 0. \end{aligned} \right\} \text{Blasiusflow} \tag{11}$$

and

$$\left. \begin{aligned} f(0) = 0, \frac{df}{d\eta}(0) = 1, \frac{df}{d\eta}(\infty) \rightarrow 0, \\ \frac{d\theta}{d\eta}(0) = -Bi[1 - \theta(0)], \theta(\infty) \rightarrow 0, \phi(0) = 1, \phi(\infty) \rightarrow 0. \end{aligned} \right\} \text{Sakiadisflow} \tag{12}$$

Table 1
Comparison of results of Eq. (6) at $M = 0, Gr = 0, Gc = 0$.

η	Parand[40]	Cortell [45]	Najafi [41]	Present [Eq. (6)]
1	0.1655724	0.16557	0.1655734	0.16557522995886
2	0.6500351	0.65003	0.6500308	0.65003502355883
3	1.3968223	1.39682	1.3968230	1.39683666515884
4	2.3057618	2.30576	2.3057710	2.30577859719202
5	3.2832910	3.28330	3.2833090	3.28330293372002
6	4.2796435	4.27965	4.2796670	4.27965257274908
7	5.2792684	5.27927	5.2792950	5.27927689321484
8	6.2792336	6.27923	6.2792810	6.27924821706894
9	7.2792358	7.27925	7.2792900	7.27925352840791

Table 2
Comparison of $f''(0)$ for Blasius equation at $M = 0, Gr = 0, Gc = 0$.

	$f''(0)$
Aminikhah [42]	0.33206
Lal and Paul [44]	0.33206
Aminikhah and Kazemi [43]	0.33206
Afridi and Qasim [46]	0.33205
Present result	0.332054275728057

Table 3
Comparison of $-\theta'(0)$ for Blasius equation at $M = 0, Gr = 0, Gc = 0$.

Bi	Aziz [13]		Subhashini et al. [24]		Present	
	Pr = 0.72	Pr = 10	Pr = 0.72	Pr = 10	Pr = 0.72	Pr = 10
0.8	0.2159	0.3812	0.21586	0.38119	0.2158635	0.38118933
1	0.2282	0.4213	0.22818	0.42134	0.2281772	0.42134193
5	0.2791	0.6356	0.27913	0.63557	0.2791296	0.63558052
10	0.2871	0.6787	0.28715	0.67873	0.2871446	0.67872083
20	0.2913	0.7026	0.29131	0.70255	0.2913272	0.70256304

where $M^2 = \frac{\sigma B_0^2 x}{\rho U_\infty}$ Magnetic field parameter, $Gr = \frac{g\beta(T_f - T_\infty)x}{U^2}$ Thermal grashof number, $Gc = \frac{g\beta_c(C_w - C_\infty)x}{U^2}$ Solutal grashof number, $Pr = \frac{\nu}{\alpha}$ Prandtl number, $Sc = \frac{\nu}{D}$ Schmidt number, $R = \frac{R_1 x}{U_\infty}$ Chemical reaction parameter, $Ec = \frac{U_\infty^2}{C_p(T_f - T_\infty)}$ Eckert number, $Bi = \frac{h_f}{k} \left(\frac{\nu x}{U_\infty}\right)^{\frac{1}{2}}$ Convective parameter

Solution procedure

Solutions of Eqs. (8)–(10) together with the boundary conditions (11) and (12) are obtained via the fourth order Runge-Kutta method with shooting technique implemented on Maple 18. The step size 0.001 is adopted to obtain the solution of the equations. The results are truncated at a distance where the boundary layers effect is less significant. The model for Blasius flows are transformed to a set of first order initial value problems as follows: Let $y_1 = f, y_2 = f', y_3 = f'', y_4 = \theta, y_5 = \theta', y_6 = \phi, y_7 = \phi'$, applying these yield

$$\left. \begin{aligned} y_1' &= y_2, y_1(0) = 0 \\ y_2' &= y_3, y_2(0) = 0 \\ y_3' &= -\frac{1}{2}y_1y_3 + M^2\sin^2(\gamma) - Gry_4 - Gcy_6, y_3(0) = s_1 \\ y_4' &= y_5, y_4(0) = 1, \\ y_5' &= -\frac{Pr}{2}(y_1y_5 - Ecy_3^2), y_5(0) = s_2, \\ y_6' &= y_7, y_6(0) = 1 \\ y_7' &= -\frac{Sc}{2}(y_1y_7 + R_1y_6), y_7(0) = s_3 \end{aligned} \right\} \tag{13}$$

To validate the solution obtained via the fourth order Runge-Kutta method, the result of $f(\eta)$ in the absence of magnetic parameter, thermal grashof number and solutal grashof number as depicted in Table 1, is compared with the ones reported in literature. Furthermore, the result of $f''(0)$ is compared with Aminikhah [42], Lal and Paul [44], Aminikhah and Kazemi [43], Afridi and Qasim [46] in Table 2. The skin friction and Nusselt number are also computed and compared, see Tables 3 and 4.

Entropy generation analysis is primarily concerned with the optimization of thermal production in fluid flow, and one of the best approaches is the application of second law of thermodynamics. Bejan [30] gave the local volumetric rate of

Table 4

Comparison of $f''(0)$ and $-\theta'(0)$ for Blasius equation for various values of Bi , Gr and Pr when $M = 0$, $Gc = 0$.

			Makinde and Olanrewaju [47]		Subhashini et al. [24]		Present	
Bi	Gr	Pr	$f''(0)$	$-\theta'(0)$	$f''(0)$	$-\theta'(0)$	$f''(0)$	$-\theta'(0)$
0.1	0.1	0.72	0.36881	0.07507	0.36875	0.07505	0.3687980	0.0750908
1.0	0.1	0.72	0.44036	0.23750	0.44032	0.23746	0.4402978	0.2375965
0.1	1.0	0.72	0.63200	0.07704	0.63198	0.07700	0.2294749	0.0770525
0.1	0.1	3.00	0.34939	0.08304	0.34937	0.08301	0.3494247	0.0830526
0.1	0.1	7.10	0.34270	0.08672	0.34270	0.08670	0.3427221	0.0867356

entropy generation as:

$$S_G = \frac{k}{T_\infty^2} \left(\frac{\partial T}{\partial y} \right)^2 + \frac{\mu}{T_\infty} \left(\frac{\partial u}{\partial y} \right)^2 + \frac{D}{C_\infty} \left(\frac{\partial C}{\partial y} \right)^2 + \frac{D}{C_\infty} \left(\frac{\partial T}{\partial y} \right) \left(\frac{\partial C}{\partial y} \right) + \frac{\sigma B_0^2}{T_\infty} u^2, \tag{14}$$

Eq. (14) gives the detailed contributions of each parameter to entropy generation. The first term on the right hand is heat transfer entropy generation, the second term is fluid friction entropy generation while the third, fourth and fifth terms are mass transfer, mass-fluid transfer and magnetic field irreversibilities respectively. Applying the similarity variables in Eqs. (7) to (14) yields

$$Ns = \left(\frac{d\theta}{d\eta}(\eta) \right)^2 + \frac{Br}{\Omega_T} \left(\frac{df}{d\eta}(\eta) \right)^2 + \lambda_1 \left(\frac{d\phi}{d\eta}(\eta) \right)^2 + \lambda_2 \left(\frac{d\theta}{d\eta}(\eta) \frac{d\phi}{d\eta}(\eta) \right) + \frac{BrM^2}{\Omega_T} \left(\frac{df}{d\eta}(\eta) \right)^2 + \frac{Br}{Da\Omega_T} \left(\frac{df}{d\eta}(\eta) \right)^2 \tag{15}$$

where $\Omega_T = \frac{T_\infty}{T_f - T_\infty}$ temperature difference parameter, $(\lambda_1 = \frac{DT_\infty^2 (C_w - C_\infty)^2}{C_\infty k (T_f - T_\infty)}, \lambda_2 = \frac{DT_\infty^2 (C_w - C_\infty)^2}{C_\infty k (T_f - T_\infty)})$ Dimensionless constant parameters, $Br = \frac{\mu U_\infty^2}{k(T_f - T_\infty)}$ Brinkman number and $Ns = \frac{\nu x T_\infty^2}{k U_\infty (T_f - T_\infty)}$ Characteristic entropy generation rate.

In Eq. (15), the characteristic entropy generation Ns is stated as the summation of irreversibilities due to heat transfer denoted as $N_1 = \left(\frac{d\theta}{d\eta}(\eta) \right)^2$ and fluid friction as

$$N_2 = \frac{Br}{\Omega_T} \left(\frac{df}{d\eta}(\eta) \right)^2 + \lambda_1 \left(\frac{d\phi}{d\eta}(\eta) \right)^2 + \lambda_2 \left(\frac{d\theta}{d\eta}(\eta) \frac{d\phi}{d\eta}(\eta) \right) + \frac{BrM^2}{\Omega_T} \left(\frac{df}{d\eta}(\eta) \right)^2. \tag{16}$$

Results and discussion

In this work, numerical solution via Runge-Kutta fourth order method with shooting technique has been proffered to the heat and mass Blasius and Sakiadis flows. The impact of themophysical parameters such as the angle of inclination, magnetic parameter, chemical reaction and Schmidt number on fluid velocity, temperature, concentration, entropy generation are discussed in plots 2–16. Realistic values of Schmidt number are chosen as follows: hydrogen ($Sc = 0.22$), water vapor ($Sc = 0.62$), ammonia ($Sc = 0.78$) and Propyl Benzene

($Sc = 2.68$) at temperature 25°C and one atmospheric pressure. Furthermore, Prandtl values number chosen is $Pr = 3$.

Figs. 2–4 depict the influence of angle of inclination α on fluid velocity, concentration and entropy generation for Blasius and Sakiadis flows. In Fig. 2A (Blasius flow) and 2B (Sakiadis flow) fluid velocity is found to have decelerated as the angle of inclination is increased. This is due to the fact that an inclined angle reinforced the decreasing effect of the magnetic field, thus retarding fluid velocity. Fig. 3A (Blasius flow) and 3B (Sakiadis flow) reveal that the influence of an inclined angle on concentration profiles is significant for both flows. In Fig. 4A (Blasius flow) entropy generation is significantly reduced, the reduction noticed is as a result of the deceleration in fluid motion as indicated in Figs. 2A, while a rise in entropy generation is displayed in Fig. 4B (Sakiadis flow).

The influence of magnetic field on fluid velocity, temperature, concentration and entropy generation for both Blasius and Sakiadis flows is presented in Figs. 5–8. Fig. 5A (Blasius flow) and 5B (Sakiadis flow) indicate a retardation in fluid motion as magnetic parameter increases in values. Application of magnetic field orthogonally to the direction of fluid flow introduces a Lorentz force, a resistive type of force which reduces fluid motion. The opposite trend is noticed in Figs. 6A and B for both Blasius and Sakiadis flows. A significant rise in fluid temperature is observed, the interaction of the applied magnetic field generated the Lorentz force which has a strong resistance to fluid motion thereby converting the kinetic energy to heat energy, that is Joule heating, hence the rise in fluid temperature. Fig. 7A (Blasius flow) and 7B (Sakiadis flow) reveal the response of concentration profile to a rise in the values magnetic parameter. Similar explanation as in Fig. 5A and B holds, the Lorentz force reduces the rate of mass transfer within the flow leading to a reduction in the concentration profile. The influence of magnetic parameter in Fig. 8A and B for Blasius and Sakiadis flows depict a considerable decline in entropy generation. The observed reduction can be traced to the net effect of the decrease in fluid velocity and concentration.

Next is the influence of chemical reaction parameter on fluid velocity, temperature, concentration and entropy generation as shown in Figs. 9–12. As depicted in Figs. 9A and 11A (Blasius flow); 9B and 11B (Sakiadis flow), a reducing trend

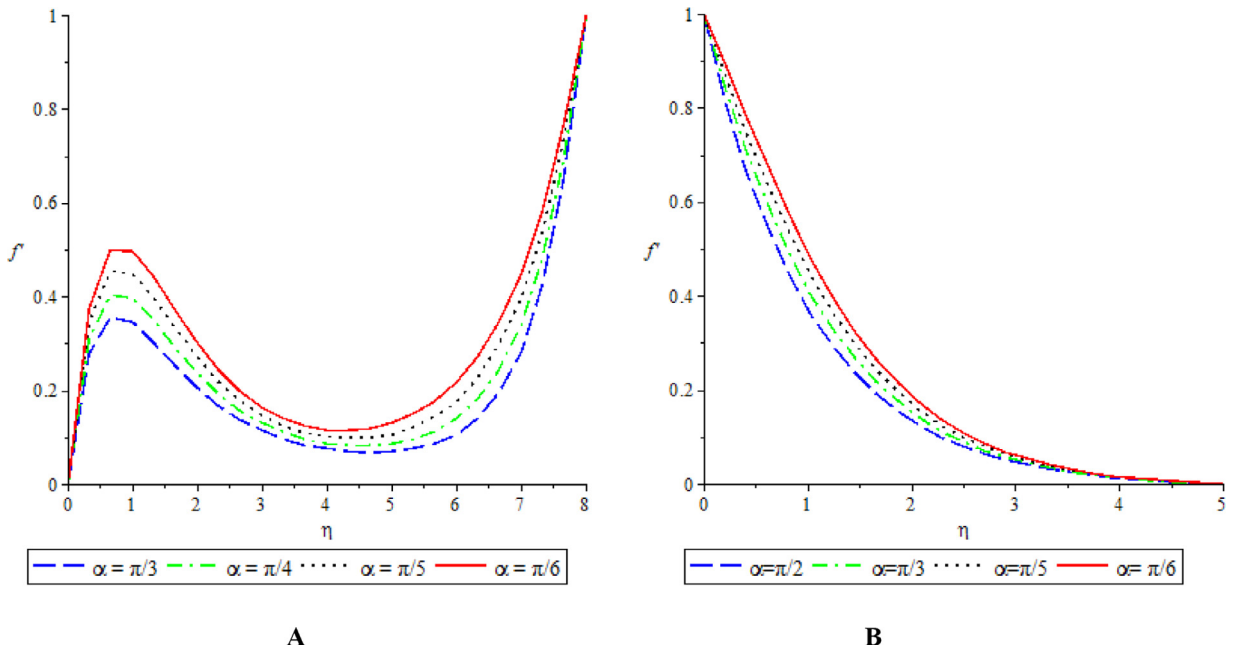


Fig. 2. α versus fluid velocity: Blasius flow (A) and Sakiadis flow (B).

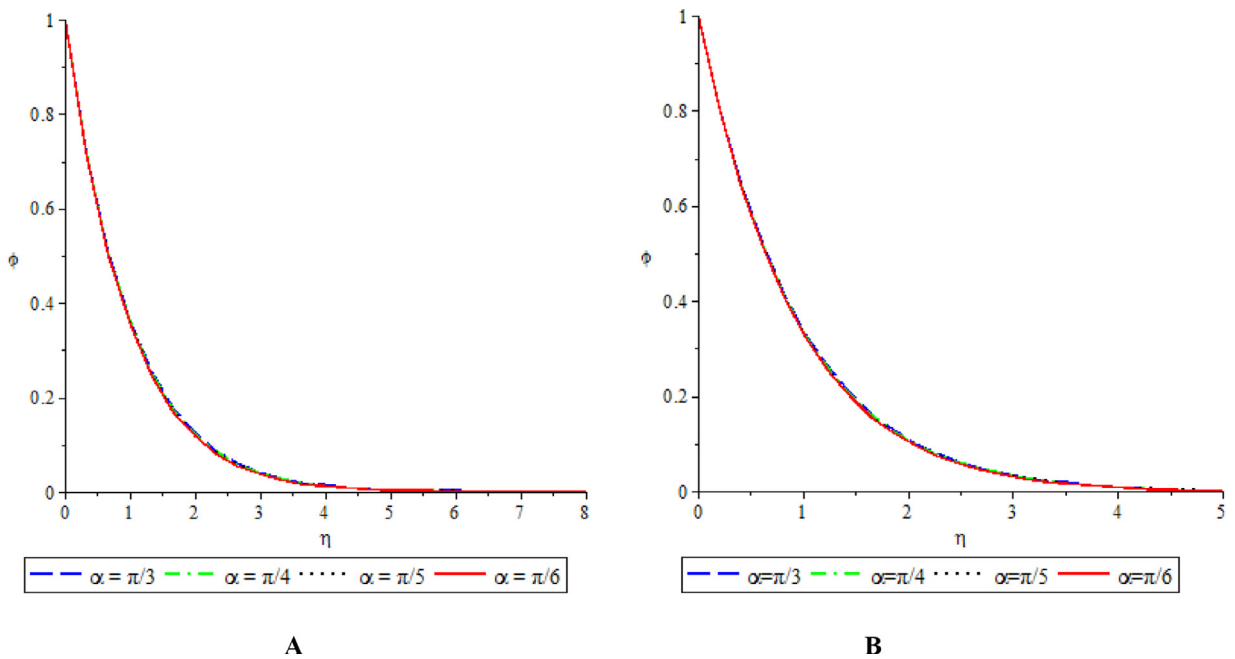


Fig. 3. α Mass Concentration: Blasius flow (A) and Sakiadis flow (B).

in velocity and concentration profiles is observed for both Blasius and Sakiadis flows as chemical reaction parameter increases in values. Destructive reaction is represented as $\gamma > 0$ while $\gamma < 0$ depicts generative reaction. The decrease noticed in Fig. 11 indicates a reduction in the thickness of solutal boundary caused by the destructive reaction as values of R rise from 1 to 7, the species concentration decreases considerably. In Figs. 10A (Blasius flow), a drop in fluid temperature is depicted while an opposite trend is noticed in Fig. 10B (Sakiadis flow) as chemical reaction parameter takes higher values. Entropy generation reduces in Fig. 12A (Blasius flow) with an increment in chemical reaction parameter while an increase in entropy generation is observed for Sakiadis flow as portrayed in Fig. 12B. The observation in Fig. 12A is an indication that chemical reaction parameter can be regulated to achieve entropy generation minimisation for Blasius.

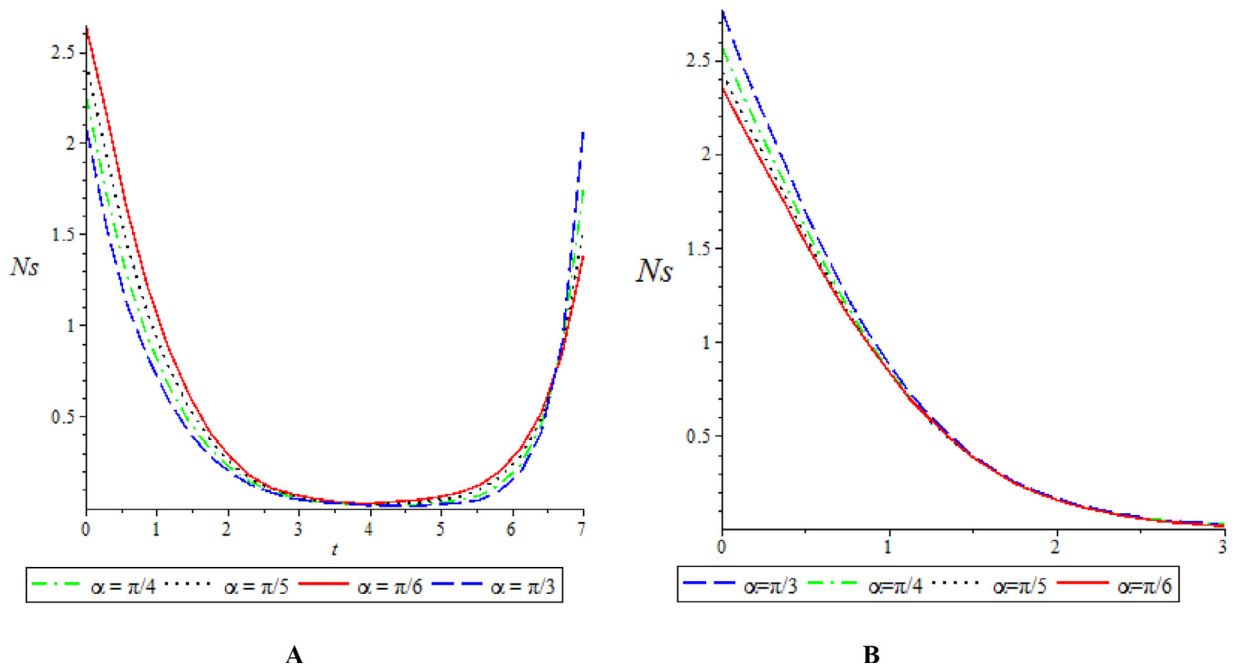


Fig. 4. α Versus Entropy Generation: Blasius flow (A) and Sakiadis flow (B).

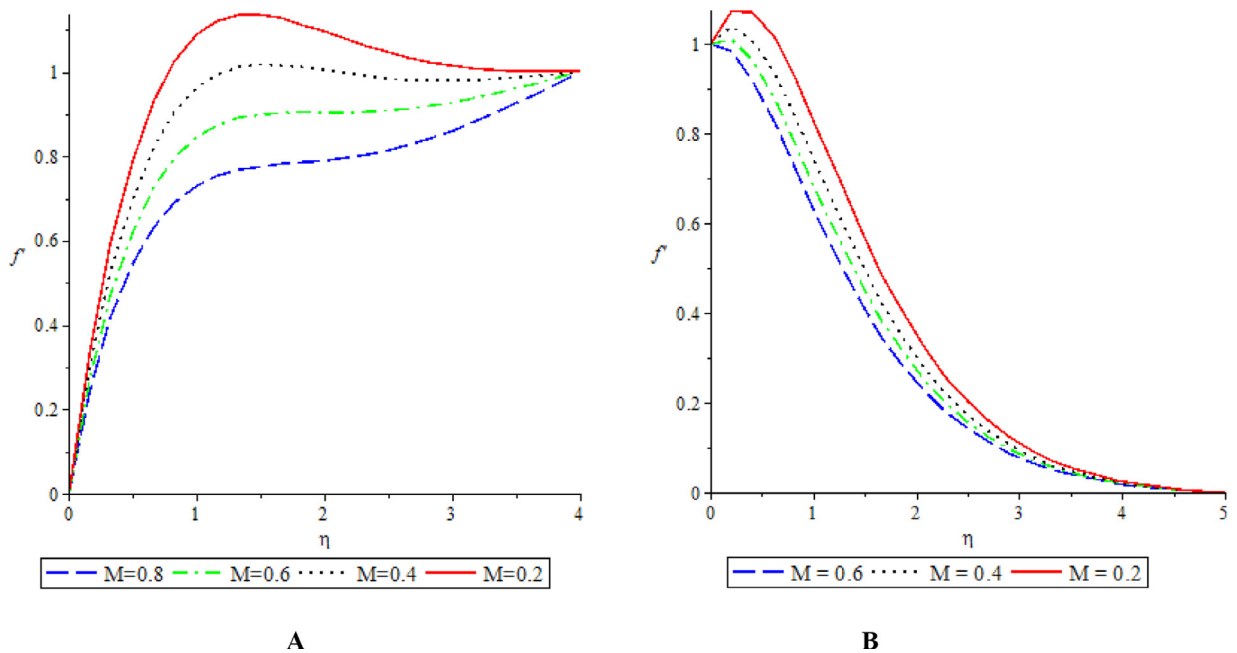


Fig. 5. M Versus Fluid Velocity: Blasius flow (A) and Sakiadis flow (B).

Finally, the plots of Schmidt versus fluid velocity, temperature, concentration and entropy generation are presented and explained in Figs. 13–16. It is evident in Figs. 13 and 15 that fluid velocity and concentration decelerate as Schmidt number increases. The term which represents Schmidt number in the concentration equation is the ratio of fluid kinematic viscosity to the mass diffusivity. It describes the relationship between the relative thickness of the hydrodynamic boundary layer and mass-transfer boundary layer, therefore a rise in Schmidt number increases fluid viscosity and reduces the species concentration leading to a fall in fluid velocity and concentration. It is also noticed in Fig. 14 that fluid temperature increases as Schmidt number increases for both Blasius flow and Sakiadis flow. Furthermore, entropy generation’s response to variation in Schmidt number is elucidated in Fig. 16A and B. In Fig. 16A entropy generation reduces for Blasius flow except in the

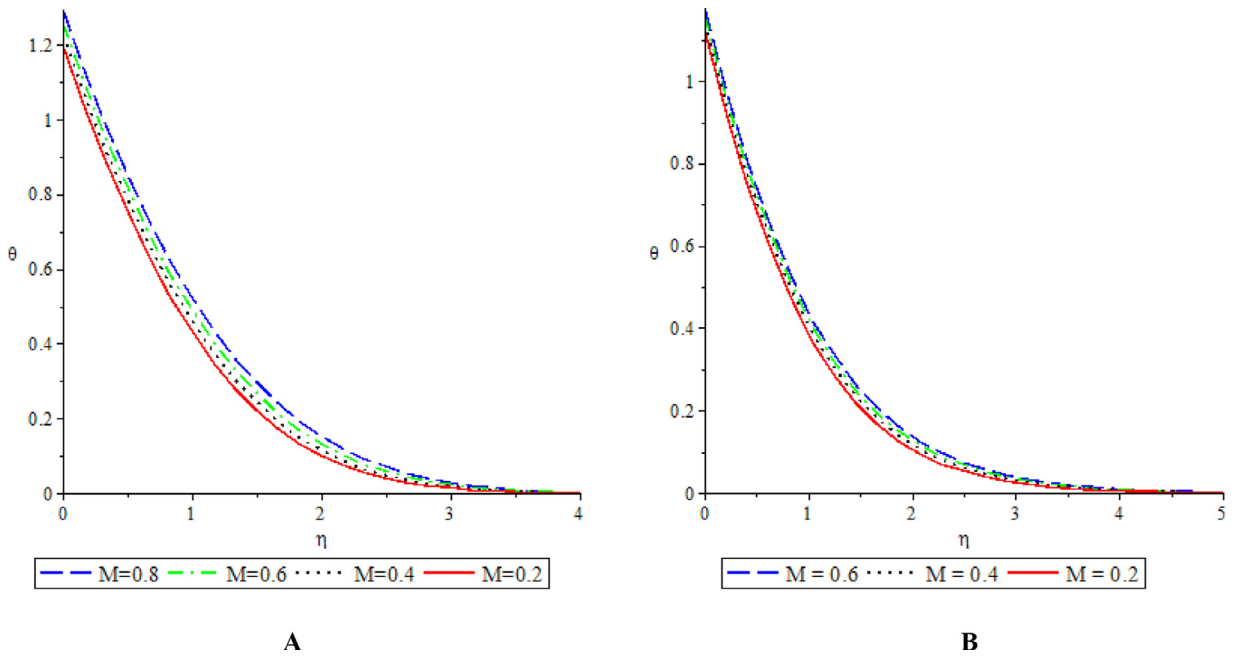


Fig. 6. M Versus Fluid Temperature: Blasius flow (A) and Sakiadis flow (B).

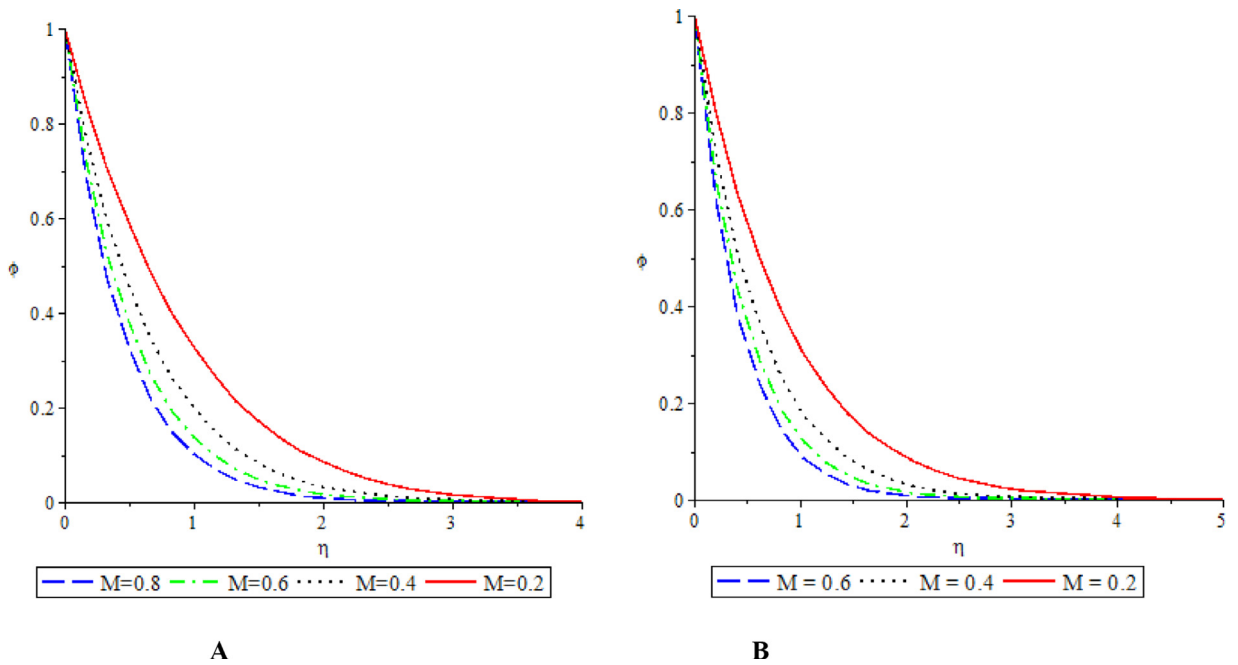


Fig. 7. M Versus Mass Concentration: Blasius flow (A) and Sakiadis flow (B).

region far away from the plate. The reason for this is linked with the observations in Figs. 13 and 14 where fluid velocity and temperature at the far away region decreases significantly. However, for Sakiadis flow as depicted in Fig. 16B entropy generation increases at the plate surface but slightly reduces in the middle of the channel.

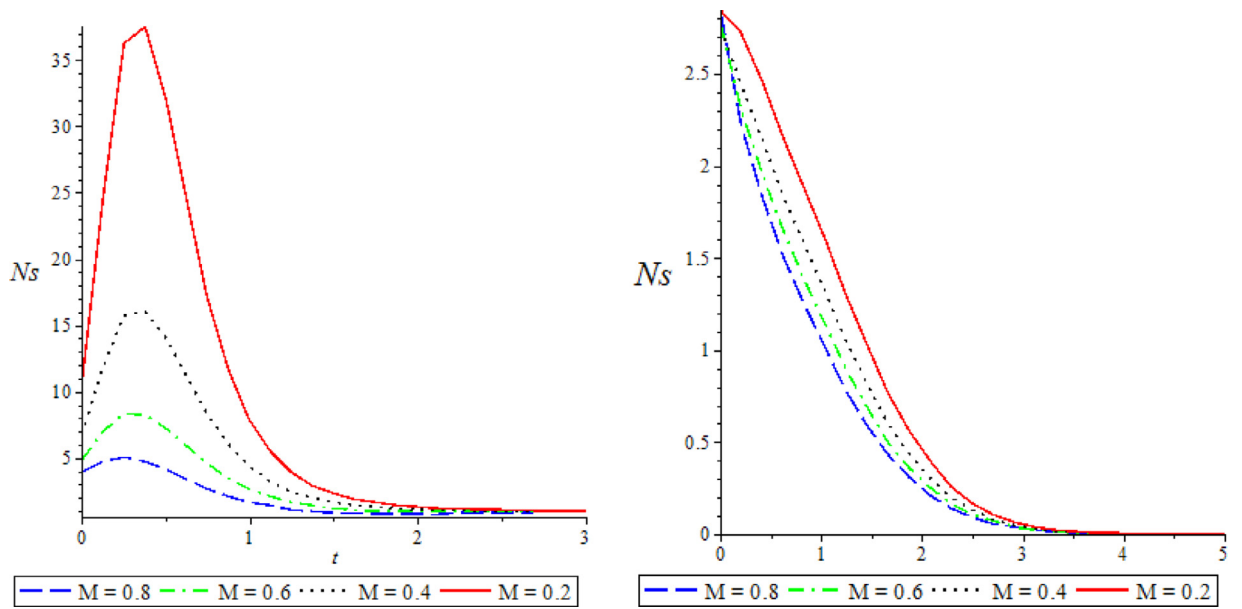


Fig. 8. M versus Entropy Generation: Blasius flow (A) and Sakiadis flow (B).

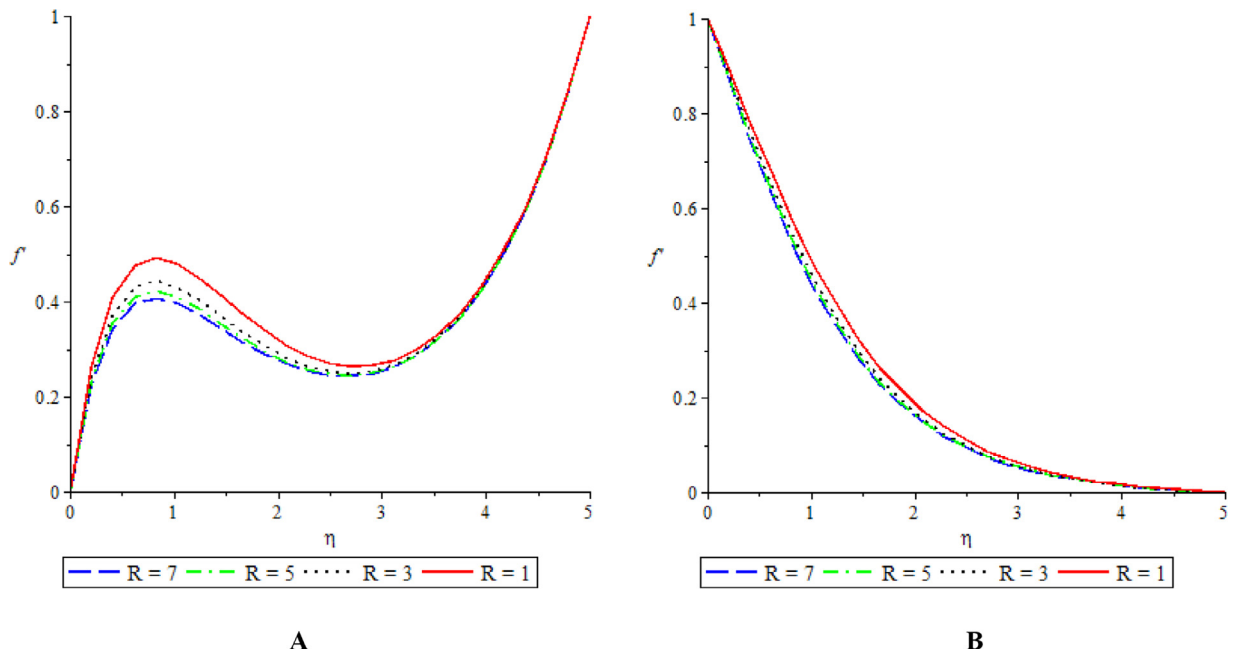


Fig. 9. R versus Fluid Velocity: Blasius flow (A) and Sakiadis flow (B).

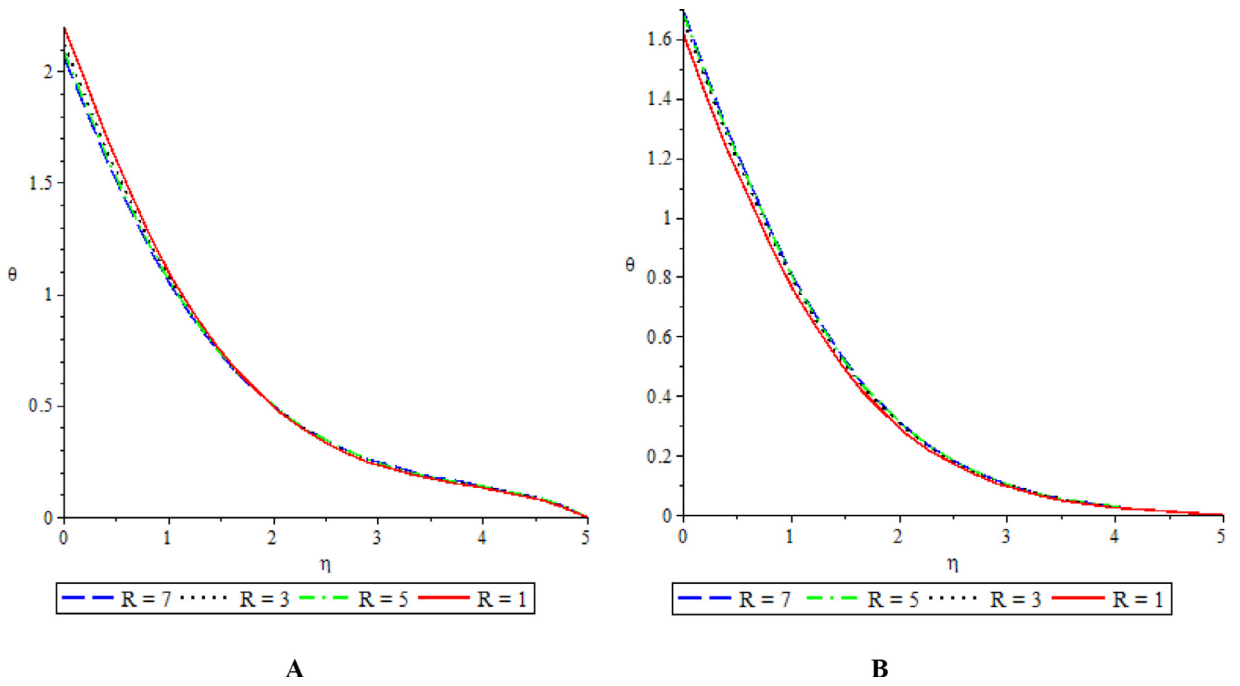


Fig. 10. R Versus Fluid Temperature: Blasius flow (A) and Sakiadis flow (B).

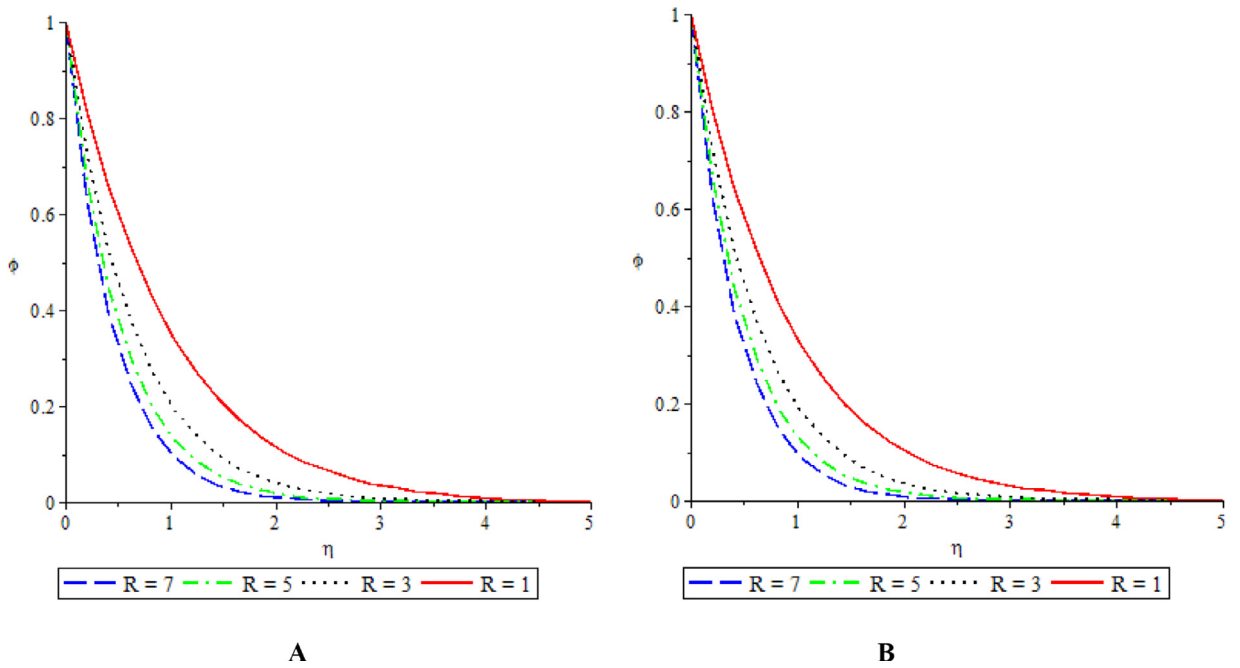


Fig. 11. R Versus Mass Concentration: Blasius flow (A) and Sakiadis flow (B).

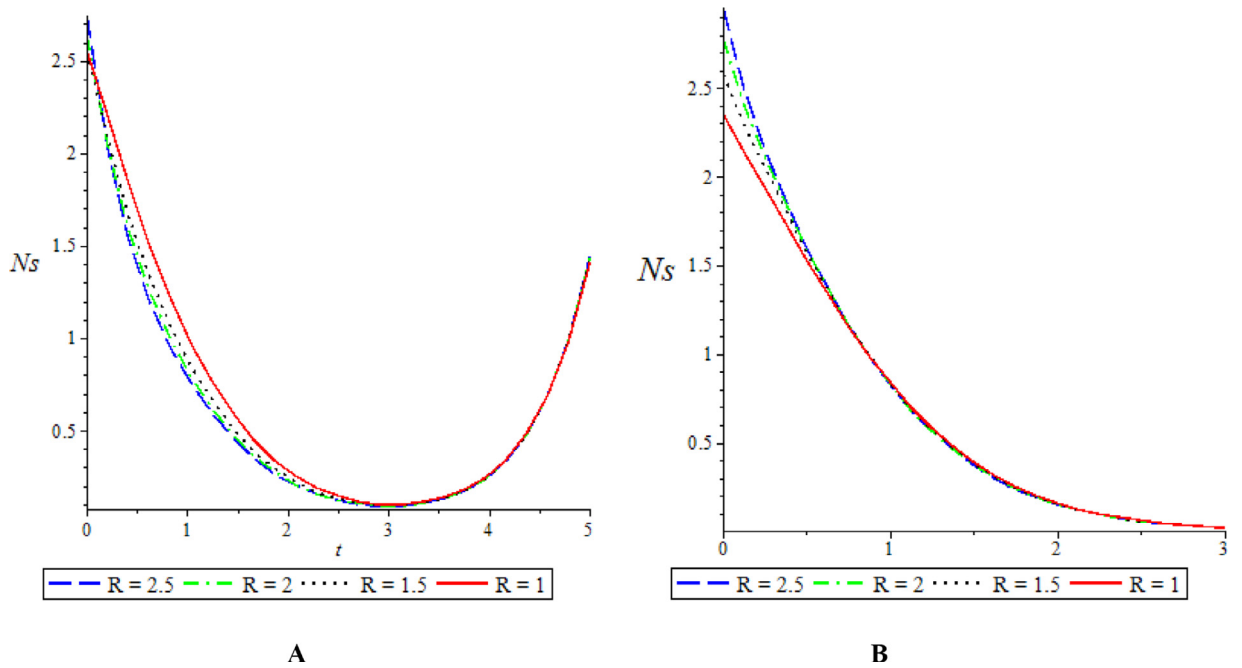


Fig. 12. R Versus Entropy Generation: Blasius flow (A) and Sakiadis flow (B).

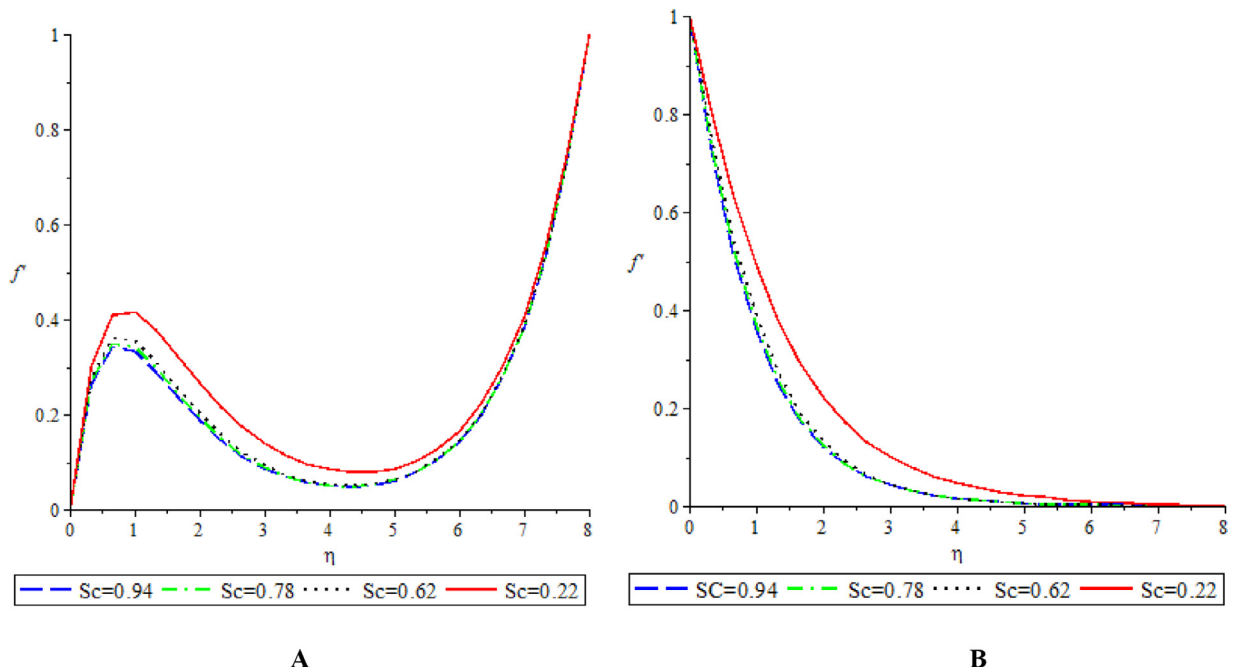


Fig. 13. Sc Versus Fluid Velocity: Blasius flow (A) and Sakiadis flow (B).

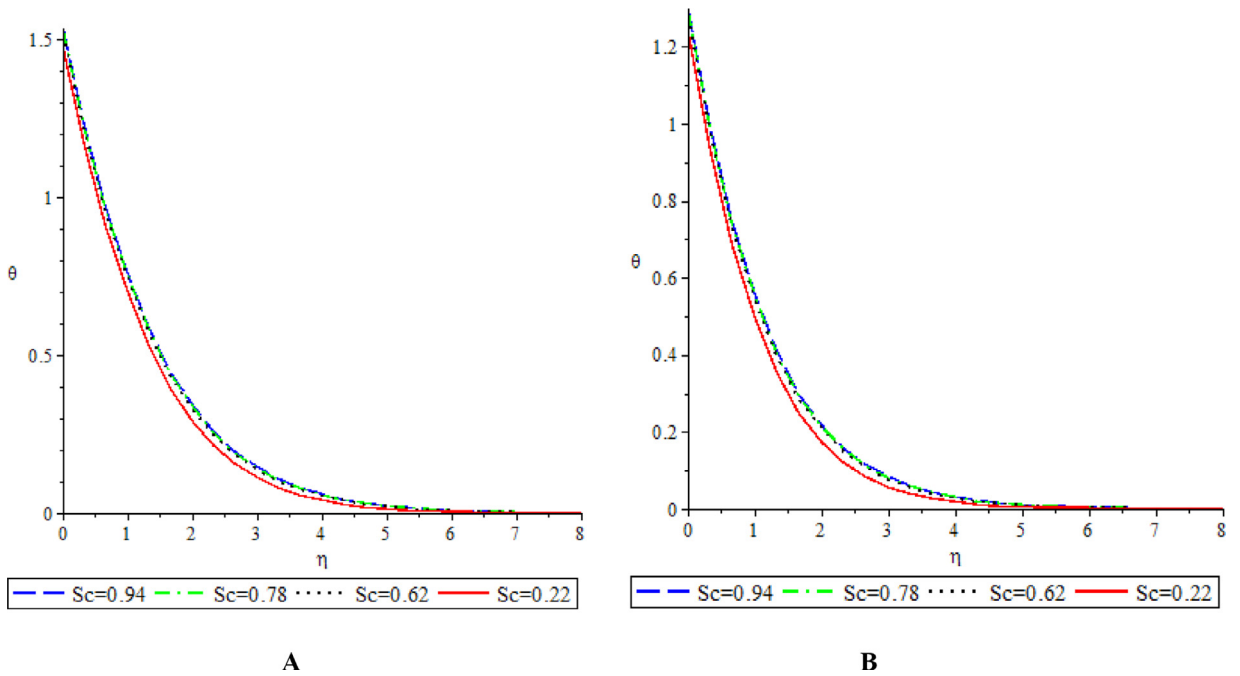


Fig. 14. ScVersus Fluid Temperature: Blasius flow (A) and Sakiadis flow (B).

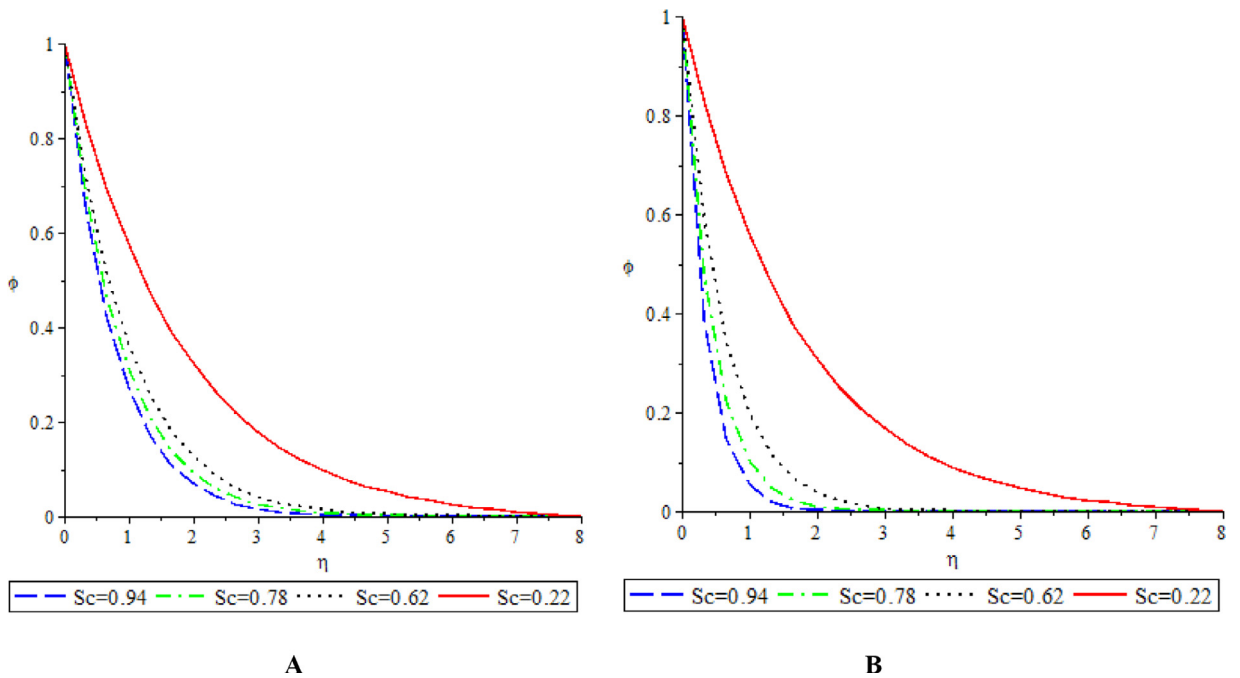


Fig. 15. ScVersus Mass Concentration: Blasius flow (A) and Sakiadis flow (B).

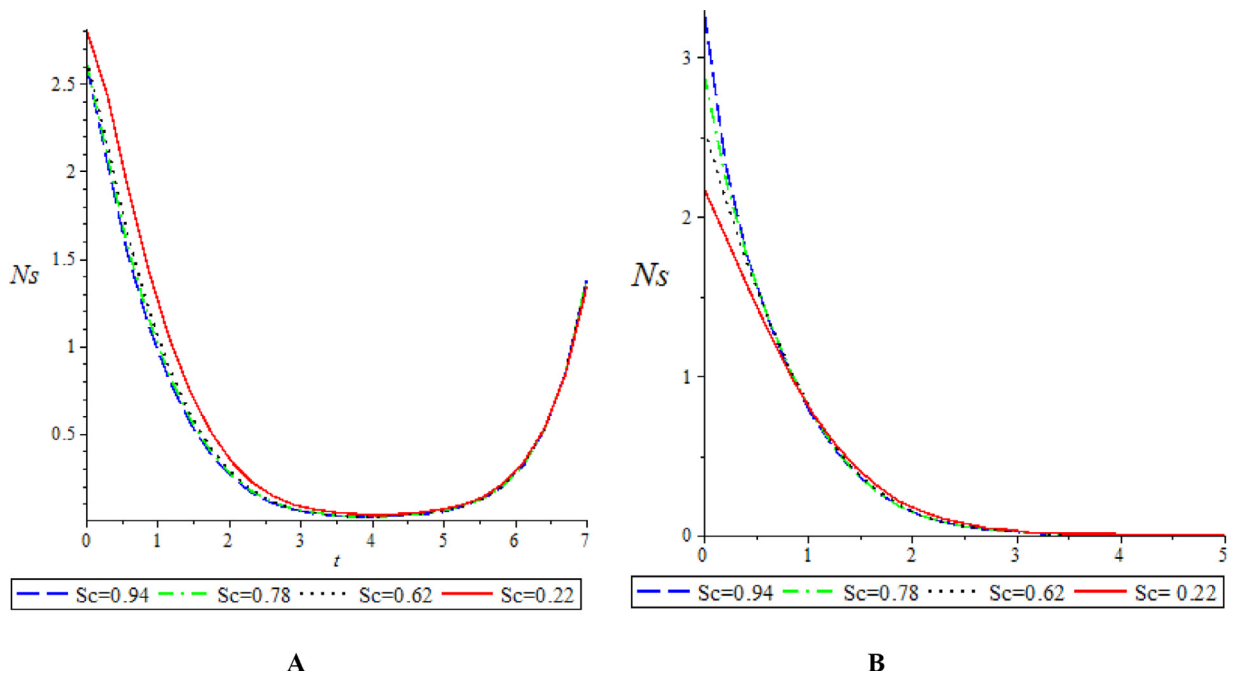


Fig. 16. Sc Versus Entropy Generation: Blasius flow (A) and Sakiadis flow (B).

Conclusion

Investigation has been conducted on the influence of inclined magnetic field and chemical reaction on the entropy generation of Blasius and Sakiadis flows. The partial differential equations that model the flows are obtained and reduced to a set of ordinary differential equations (ODE). The numerical solutions of velocity, temperature and concentration profiles are obtained via the fourth order Runge-Kutta method with the shooting technique by transforming the ODE into a set of initial value problems. The results are employed to compute entropy generation. The following submissions based on the results are given:

- 1 Fluid velocity decelerates for both Blasius and Sakiadis flows with increase in inclined parameter, magnetic parameter, chemical reaction parameter and Schmidt number,
- 2 Fluid temperature receives a boost for Blasius and Sakiadis flows as the values of magnetic parameter, chemical reaction parameter (except for Blasius flow) and Schmidt number increase,
- 3 Fluid concentration decays for Blasius and Sakiadis flows with variation in magnetic field parameter, chemical reaction parameter and Schmidt number,
- 4 For Blasius flow, entropy generation drops considerably with increases in magnetic parameter, chemical reaction parameter and Schmidt number,
- 5 For Sakiadis flow, entropy generation increases at the plate surface with increase in Inclined angle, chemical reaction parameter and Schmidt number.

The result of entropy generation for the Blasius flow is an indication that these parameters can be adjusted to control fluid irreversibility. This investigation gives more insight into the entropy generation minimisation (EGM) regime. It is revealed that appropriate values of some flow parameters such as inclined parameter, magnetic parameter, chemical reaction parameter and Schmidt number can be chosen to minimise entropy generation rate. Therefore efficient utilisation of available resources and optimal design is realisable.

Declaration of Competing Interest

The authors declare that there is no conflict of interest and have received no specific funding for this work

Acknowledgement

The authors are grateful to [Covenant University Centre for Research, Innovation and Discovery \(CUCRID\)](#) for financial support.

References

- [1] H. Blasius, Grenzsichten in Flussigkeiten mit kleiner reibung, *Z. Math Phys.* 56 (1908) 1–37.
- [2] B.C. Sakiadis, Boundary-layer behavior on continuous solid surfaces: boundary-layer equations for two-dimensional and axisymmetric flow, *AIChE J.* 7 (1961) 26–28.
- [3] L. Howarth, On the solution of the laminar boundary layer equations, *Proc. Lond. Math. Soc. A* 164 (1938) 547–579 <http://dx.doi.org/10.1098/rspa.1938.0037>.
- [4] A.M.M. Abussita, A note on a certain boundary layer equation, *Appl. Math. Comput.* 64 (1994) 73–77.
- [5] M.J. Lighthill, *Proc. R. Soc. Lond. A* 202 (1950) 359.
- [6] F.K. Tsou, E.M. Sparrow, R.J. Goldstein, Flow and Heat transfer in the boundary layer on a continuous moving surface, *Int J Heat Mass Transf* 10 (1967) 281–288.
- [7] C.H. Chen, Forced convection over a continuous sheet with suction or injection moving in a flowing fluid, *Acta Mech.* 138 (1999) 1–11.
- [8] M.A. Hossain, K. Khanafer, K. Vafai, The effect of radiation on free convection flow of fluid with variable viscosity from a porous vertical plate, *Int. J. Therm. Sci.* 40 (2001) 115–124.
- [9] A. Raptis, C. Perdiki, H.S. Takhar, Effect of thermal radiation on MHD flow, *Appl. Math. Comput.* 153 (2004) 645–649.
- [10] R.C. Bataller, Radiation effects in the Blasius flow, *Appl. Math. Comput.* 198 (1) (2008) 333–338.
- [11] P.O. Olanrewaju, J.A. Gbadeyan, O.O. Agboola, S.O. Abah, Radiation and viscous dissipation effects for the Blasius and Sakiadis flows with a convective surface boundary condition, *Int. J. Adv. Sci. Technol.* 2 (4) (2011) 102–155.
- [12] R.C. Bataller, radiation effects for the blasius and sakiadis flows with a convective surface boundary condition, *Appl. Math. Comput.* 206 (2008) 832–840.
- [13] A. Aziz, A similarity solution for laminar thermal boundary layer over a flat plate with a convective surface boundary condition, *Commun. Nonlinear Sci. Numer. Simul.* 14 (2009) 1064–1068.
- [14] T. Fang, Similarity solutions for a moving-flat plate thermal boundary layer, *Acta Mech.* 163 (2003) 161–172.
- [15] A.S. Butt, S. Munawar, A. Ali, A. Mehmood, Entropy generation in hydrodynamic slip flow over a vertical plate with convective boundary, *J. Mech. Sci. Technol.* 26 (9) (2012) 2977–2984.
- [16] S.P.A. Devi, P. Suriyakumar, Effect of magnetic field on Blasius and Sakiadis flow of nanofluids past an inclined plate, *J. Taibah Univ. Sci.* (2017) <http://dx.doi.org/doi; doi:10.1016/j.jtusc.2017.03.004>.
- [17] O. Aydin, A. Kaya, MHD mixed convective heat transfer about an inclined plate, *Heat Mass Transf.* 46 (2009) 129–136.
- [18] M. Waqas, A mathematical and computational framework for heat transfer analysis of ferromagnetic non-Newtonian liquid subjected to heterogeneous and homogeneous reactions, *J. Magn. Magn. Mater.* (2020) 493 <https://doi.org/10.1016/j.jmmm.2019.165646>.
- [19] M. Waqas, W.A. Khan, Z. Asghar, An improved double diffusion analysis of non-Newtonian chemically reactive fluid in frames of variables properties, *Int. Commun. Heat Mass Transf.* (2020) 115 <https://doi.org/10.1016/j.icheatmasstransfer.2020.104524>.
- [20] M. Waqas, S. Naz, T. Hayat, M.I. Khan, A. Alsaedi, Hydromagnetic Carreau nanoliquid in frames of dissipation and activation energy, *Commun. Theor. Phys.* 71 (2019) 14–16.
- [21] M. Waqas, S. Jabeen, T. Hayat, S.A. Shehzad, A. Alsaedi, Numerical simulation for nonlinear radiated Eyring-Powell nanofluid considering magnetic dipole and activation energy, *Int. Commun. Heat Mass Transf.* (2020) 112 <https://doi.org/10.1016/j.icheatmasstransfer.2019.104401>.
- [22] T. Hayat, M. Waqas, S.A. Shehzad, A. Alsaedi, Effects of Joule heating and thermophoresis on the stretched flow with convective boundary condition, *Sci. Iran. B* 21 (3) (2014) 682–692.
- [23] T. Hayat, M. Waqas, S.A. Shehzad, A. Alsaedi, Chemically reactive flow of third grade fluid by an exponentially convected stretching sheet, *J. Mol. Liq.* 223 (2016) 853–860 <https://doi.org/10.1016/j.molliq.2016.09.007>.
- [24] S.V. Subhashini, N. Samuel, I. Pop, Double-diffusive convection from a permeable vertical surface under convective boundary condition, *Int. Commun. Heat Mass Transf.* 38 (2011) 1183–1188.
- [25] P. Reddaiah, D.R.V.P. Rao, Convective heat and mass transfer flow of a viscous fluid through a porous medium in an duct-by finite element method, *Int. J. Appl. Math. Mech.* 8 (10) (2012) 1–27.
- [26] P.O. Olanrewaju, F.I. Alao, A. Adeniyi, S.A. Bishop, Double-diffusive convection from a permeable vertical surface under convective boundary condition in the presence of heat generation and thermal radiation, *Nonlinear Sci. Lett. A* 4 (3) (2013) 76–90.
- [27] T. Hayat, M. Waqas, S.A. Shehzad, A. Alsaedi, Mixed convection flow of a Burgers nanofluid in the presence of stratifications and heat generation/absorption, *Eur. Phys. J. Plus* 131 (253) (2016) <https://doi.org/10.1140/epjp/i2016-16253-9>.
- [28] M. Irfan, M.S. Anwar, M. Rashid, Arrhenius activation energy aspects in mixed convection Carreau nanofluid with nonlinear thermal radiation, *Appl. Nanosci.* (2020) <https://doi.org/10.1007/s13204-020-01498-5>.
- [29] A. Bejan, A study of entropy generation in fundamental convective heat transfer, *J. Heat Transf.* 101 (1979) 718–725.
- [30] Bejan A. (1996) Entropy Generation Minimization. CRC Press, USA.
- [31] S.O. Adesanya, Second law analysis for third-grade fluid with variable properties, *J. Thermodyn.* (2014) <http://dx.doi.org/10.1155/2014/452168>.
- [32] S.O. Adesanya, O.D. Makinde, Effects of couple stresses on entropy generation rate in a porous channel with convective heating, *Comput. Appl. Math.* 34 (2015) 293–307, doi:10.1007/s40314-014-0117-z.
- [33] S. Das, S. Chakraborty, R.N. Jana, O.D. Makinde, Entropy analysis of unsteady magneto-nanofluid flow past accelerating stretching sheet with convective boundary condition, *Appl. Math. Mech.* 36 (2015) 1593–1610.
- [34] W.A. Khan, R. Culham, A. Aziz, Second law analysis of heat and mass transfer of nanofluids along a plate with prescribed surface heat flux, *ASME J. Heat Transf.* 137 (8) (2015) <https://doi.org/10.1115/1.4030246>.
- [35] A. Khan, I. Khan, F. Ali, S. Shafie, A note on entropy generation in MHD flow over a vertical plate embedded in a porous medium with arbitrary shear stress and ramped temperature, *J. Porous Media* 19 (2) (2016) 175–187.
- [36] M.Q.A. Odat, R.A. Damseh, M.A.A. Nimr, Effect of magnetic field on entropy generation due to laminar forced convection past a horizontal flat plate, *Entropy* 4 (2004) 293–303.
- [37] A.A. Opanuga, O.O. Agboola, J.A. Gbadeyan, H.I. Okagbue, Entropy generation analysis of Hall current effect on MHD micropolar fluid flow with rotation effect, *SN Appl. Sci.* (2020) <https://doi.org/10.1007/s42452-019-1783-7>.
- [38] A.A. Opanuga, J.A. Gbadeyan, O.O. Agboola, H.I. Okagbue, Effect of suction/injection on the entropy generation of third grade fluid with convective cooling, *Defect Diffus. Forum* 384 (2018) 465–474.
- [39] A.A. Opanuga, J.A. Gbadeyan, S.A. Iyase, Second law analysis of hydromagnetic couple stress fluid embedded in a non-Darcian porous medium, *IAENG Int. J. Appl. Math.* 47 (3) (2017) 287–294.
- [40] K. Parand, A. Taghavi, Rational scaled generalized Laguerre function collocation method for solving the Blasius equation, *J. Comput. Appl. Math.* 233 (2009) 980–989.
- [41] E. Najafi, Numerical quasilinearization scheme for the integral equation form of the Blasius equation, *Comput. Methods Differ. Equ.* 6 (2018) (2018) 141–156.
- [42] H. Aminikhah, Analytical approximation to the solution of nonlinear Blasius' viscous flow equation by LTNHMP, *ISRN Math. Anal.* (2012) <https://doi.org/10.5402/2012/957473>.
- [43] H. Aminikhah, S. Kazemi, Numerical solution of the Blasius viscous flow problem by quartic B-spline method, *Int. J. Eng. Math.* (2016) (2016) <https://doi.org/10.1155/2016/9014354>.
- [44] S.A. Lal, N.M. Paul, An accurate Taylors series solution with high radius of convergence for the Blasius function and parameters of asymptotic variation, *J. Appl. Fluid Mech.* 7 (2014) 557–564.

- [45] R. Cortell, Numerical solutions of the classical Blasius flat-plate problem, *Appl. Math. Comput.* 170 (2005) 706–710.
- [46] M.I. Afridi, M. Qasim, Second law analysis of Blasius flow with nonlinear Rosseland thermal radiation in the presence of viscous dissipation, *Propuls. Power Res.* 8 (3) (2019) 234–242.
- [47] O.D. Makinde, P.O. Olanrewaju, Buoyancy effects on thermal boundary layer over a vertical plate with a convective surface, *ASME, J. Fluid Eng.* 132 (044502) (2010) 1–4.